Preprint version of the article: S. R. Nekoo and A. Ollero, "A Proportional Closed-loop Control for Equivalent Vertical Dynamics of Flapping-Wing Flying Robot," 2023 International Conference on Unmanned Aircraft Systems (ICUAS), Warsaw, Poland, 2023, pp. 1294-1300, doi: 10.1109/ICUAS57906.2023.10156070.

A Proportional Closed-loop Control for Equivalent Vertical Dynamics of Flapping-Wing Flying Robot

Saeed Rafee Nekoo and Anibal Ollero
GRVC Robotics Lab., Departamento de Ingeniería de Sistemas y Automática
Escuela Técnica Superior de Ingeniería, Universidad de Sevilla, Seville, Spain
Emails: saerafee@yahoo.com, aollero@us.es
ORCID: 0000-0003-1396-5082, 0000-0003-2155-2472

***Abstract*—The closed-loop position control of a flapping-wing flying robot (FWFR) is a challenging task. A complete six-degree-of-freedom (DoF) modeling and control design is preferable though that imposes complexity on the procedure and analysis of the oscillations in the trajectory. Another approach could be studying independent state variables of the system and designing a controller for them. This will provide the possibility of a better understanding of the dynamic, comparing to experimental data, then use this information for moving forward to complete 6-DoF modeling. In this work, a simple linear proportional closed-loop controller is proposed and analyzed for an equivalent dynamic model of the flapping-wing flying robot. The equivalent dynamic modeling considers the flapping motion as a base excitation that disturbs the system in oscillatory behavior. The frequency of the oscillation and data of the motion was obtained from previous experimental results and used in the modeling. The designed controller performed the regulation task easily and regulated the system to a series of set-point control successfully. The motivation for the selection of a proportional control is to keep the design as simple as possible to analyze the excitation and behavior of the flapping more precisely. A discussion on the transient and steady-state flight and the role of control design on them have been presented in this work.**

Keywords*—Proportional control, Flapping-wing, Aerial robotics, Closed-loop design, Base-excitation.

I. INTRODUCTION

Flapping-wing flying robots (FWFRs) have become interesting and challenging case studies in robotics. A part of the recent development in flapping-wing systems focused on closed-loop position control. The precise control is a necessary step of various applications for FWFRs such as perching on a branch [1], perching to a surface [2, 3], vision-based monitoring systems [4-8], long-endurance flights [9, 10], manipulation [11, 12], etc. The system in question is under-actuated and the control inputs could be the frequency of the flapping, and the motion of the tails. Full control capability over this under-actuated system is difficult. There were valuable studies to design several control methods to achieve a closed-loop stable regulation, briefly reviewed in the following. A dihedral-based control was introduced and experimented with a flapping-wing small aircraft [13]. The robot flew in gliding mode and the application of the flight was perching (landing) on a surface. Fei et al. presented flight control in a hovering condition and trajectory tracking for a tailless flapping-wing robot using a robust closed-loop feedback control [14]. Gao et al. investigated the adaptive control of bionic flapping wings using a neural network approach [15]. Adaptive nonlinear control was also exercised for the gliding phase of an FWFR for perching application [16]. The perching in the gliding phase does not suffer from the oscillation of the flapping, approximately $10(\mathrm{cm})$ disturbance to the trajectory, and motivated the designers to use this phase of flight for that application.

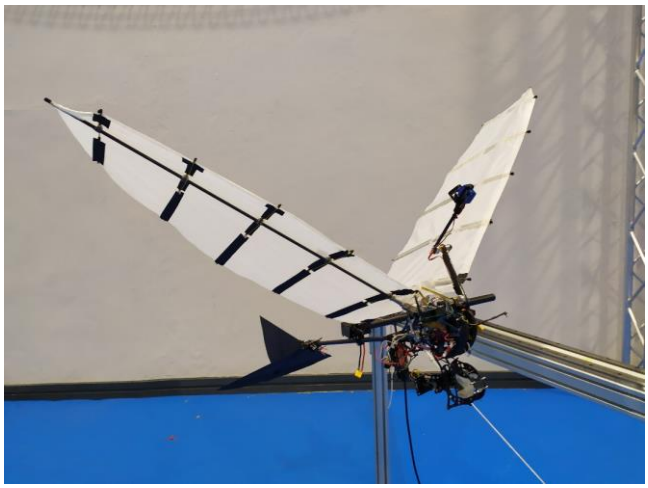

Fig. 1. The E-Flap prototype, mounted on the launcher; claw below the robot, and the manipulator on top.

The challenge in control is rooted in the limited number of actuators, availability of position feedback, design, and manufacturing and one of the most difficult one is the limited payload. The limited payload capacity forces the designs to be very lightweight resulting in fragile mechanisms with limited inputs, i.e. the E-Flap possessed a flapping wing, rudder, and elevator in the tail as the inputs (three inputs in total) [17]. With that configuration, the forward flight is always needed. In a simulation environment, more actuators were added to control flapping-wing systems; however, the possibility of prototyping and real flight with those complex configurations is a question [18].

Closed-loop position control using a combination of linear controllers was successfully experimented with in an indoor environment for E-Flap [1]. The feedback to the bird was the 3D position of the robot and its orientation, provided by an Opti-track motion-capture system. The limitation on the

Preprint version of the article: S. R. Nekoo and A. Ollero, "A Proportional Closed-loop Control for Equivalent Vertical Dynamics of Flapping-Wing Flying Robot," 2023 International Conference on Unmanned Aircraft Systems (ICUAS), Warsaw, Poland, 2023, pp. 1294-1300, doi: 10.1109/ICUAS57906.2023.10156070.

forward flight was still applicable which led to an impact to the branch for perching with almost $2\left(\frac{\mathrm{m}}{\mathrm{s}}\right)$ [1]. The speed of forward flight was recorded in the range of $v_x \in [2,8]\left(\frac{\mathrm{m}}{\mathrm{s}}\right)$, an initial speed of launching (less than 4), a flight between 4 to 8, and a lowering speed for perching around 2. The frequency of the flapping is one of the most important sources of speed and height control in flights. There was also evidence of forced oscillations to the robot by the flapping action, visible in the flight data, in Z-axis direction. This vertical oscillation motivated us to model and study the effect of the base excitation and consequently design an independent control for that. The set of linear controllers in [1], was also decoupled so, this will help us to present a more accurate flight controller for future experimentation.

Base excitation is a well-known phenomenon in mechanical vibration [19, 20]. The application is quite diverse and some examples could be named such as the analysis of fluid in pipes [21], energy harvesting in cantilever beams [22], piezoelectric stack energy harvester [23], dynamic analysis of laminated composite material [24], and many more. The modeling of base excitation helps a designer choose the proper damping coefficient, elastic constant, and frequency of the excitation to put the system in a safe zone to avoid possible resonance or other destructive effects. Müller et al. used this concept to define damping value from data of phase resonance in a system subjected to base excitation [19].

Here in this work, the frequency of the flapping is modeled as a forced excitation to the base and it provides the power of flight so it cannot be omitted. The logical approach is to define the flapping limits in a zone that provides enough lift force without damaging the system, which motivates modeling, simulation, and analysis such as this work. The modeling and control will help us to set the elastic constant and damping coefficient in a zone that provides a sufficiently smooth condition for flight and acceptable precision in position control. For this work, a simple proportional (P) closed-loop linear controller has been chosen to present a clear analysis on the part of oscillation and base excitation and also provide valuable inputs for future modifications on the available linear controller on the E-Flap prototype. A discussion on the transient and steady-state flight has been provided to show the reason for choosing this P controller. The limited zone of experimentation forced the flight to be in the transient zone of regulation; so, moving towards complex control at this stage might not be reasonable, as discussed in Section IV.

The main contribution of this work is to model and control the elevation (control in Z-axis) of the flapping-wing flying robot, considering the oscillation of the flapping wings as the excitation of the base.

The remainder of the work includes: Section II presents the system modeling and dynamics of the base excitation system. Section III expresses the control design and defines the parameters of the robot. Section IV is devoted to simulation results and Section V states the concluding remarks.

II. System Modelling and Dynamics of Base Excitation

The flapping-wing robot for vertical base-excitation modeling is F-Flap [17], originally weighed $500(\mathrm{g})$ with the possibility of almost $500(\mathrm{g})$ more load-carrying capacity. The addition of a leg to the system increased the weight to $700(\mathrm{g})$ including a line sensor and additional servomotor for activating the leg [1]. The current version, represented in Fig. 1, has also an additional $79(\mathrm{g})$ two-DoF manipulator [11].

Despite the changes in the weight of the system and configuration of the add-ons such as manipulator, camera, and leg, there have been always oscillations in the motion control in Z-axis direction, see Fig. 2, which shows a set of flight data with different set points as an example. These oscillations were caused by the main actuator of the robot, the flapping wing, and vary in the range of $[3.5,4.5](\mathrm{Hz})$ [17]. The limit was set to have a minimum thrust force for moving forward and a lift force to keep the robot steadily flying in the air. The maximum limit also avoids the wing to be damaged by the high produced force. The range will be used in this work to define the limits of the proportional gain and the controller.

Assumption 1. The frequency of the flapping is limited to $[3.5,4.5](\mathrm{Hz})$ which is sufficient to change the altitude of the flapping wing robot.

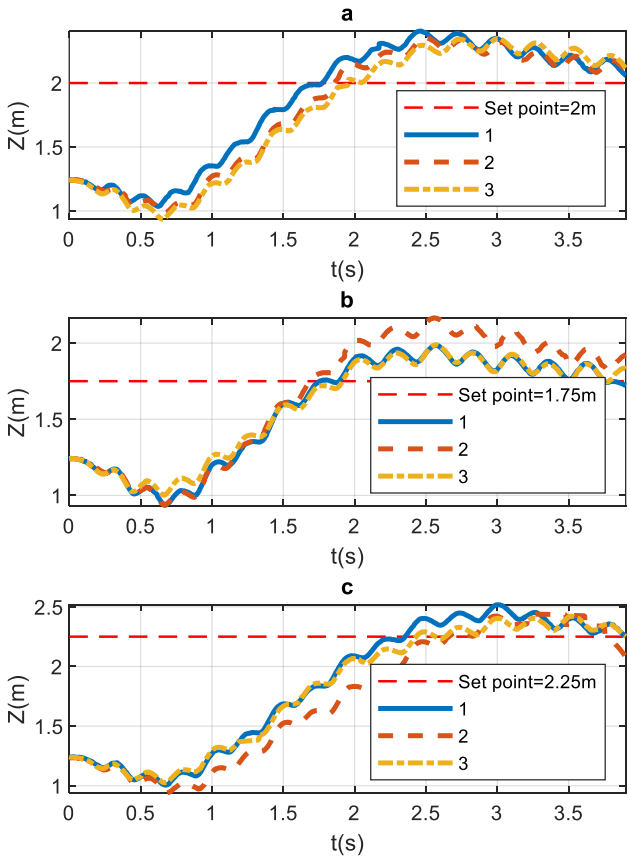

Fig. 2. Regulation and behavior of the flapping-wing robot in vertical motion for a series of experiments, a series of flight as an example, more data of flight are available though the behavior of the oscillation is the same [1].

Preprint version of the article: S. R. Nekoo and A. Ollero, "A Proportional Closed-loop Control for Equivalent Vertical Dynamics of Flapping-Wing Flying Robot," 2023 International Conference on Unmanned Aircraft Systems (ICUAS), Warsaw, Poland, 2023, pp. 1294-1300, doi: 10.1109/ICUAS57906.2023.10156070.

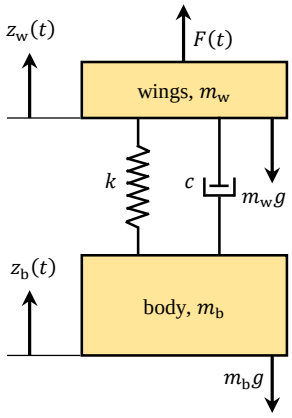

Fig. 3. The presentation of the equivalent dynamic with base excitation.

The other two actuators are the rudder and elevator of the tail, responsible for yaw and pitch control respectively. Both actuators of the tail will indeed have interactions on other degrees of freedom, but for the sake of simplicity in the modeling, it will be assumed that the interactions are negligible. An example is that the elevator of the tail changes the pitch and the pitch angle changes the lift force of the wings, which is the cause of ascending or descending of the robot. To make the modeling valid, it is assumed that the robot flies with a steady value for the elevator (that means a constant pitch angle). Then the frequency of flapping will increase or decrease the height of the FWFR in flight.

Assumption 2. The robot flies with negligible change in the pitch angle, then the role of flapping frequency is dominant in the change of the altitude.

With the mentioned assumptions, the robot could be modeled as a mechanical system with two parts: body and wings, see Fig. 3. The body plays the role of the base and the wings are generating the excitation to the base.

Considering the free-body-diagram in Fig. 3, the equation of motion of the system is written as:

$$\begin{aligned} m_b\ddot{z}_b(t) + c\dot{z}_b(t) + kz_b(t) + (m_b + m_w)g \\ = m_w\ddot{z}_w(t) + c\dot{z}_w(t) + kz_w(t) \\ + \bar{F}(t), \end{aligned} \tag{1}$$

where m_b and m_w(kg) are mass of base and wings respectively, c(Ns/m) is damping coefficient, k(N/m) is stiffness coefficient, $z_b(t) \in \mathbb{R}$ is a generalized coordinate of the system and $z_w(t) \in \mathbb{R}$ is the excitation of the base and $g = 9.81(\mathrm{m/s^2})$ is the gravity constant. $\bar{F}(t) \in \mathbb{R}$ is an input lift force produced by flapping. The excitation of the base and its derivatives are introduced as

$$\begin{aligned} z_w(t) &= z_0 \sin(\omega(t)t), \\ \dot{z}_w(t) &= z_0\{\omega(t) + \dot{\omega}(t)t\}\cos(\omega(t)t), \\ \ddot{z}_w(t) &= z_0[\{2\dot{\omega}(t) + \ddot{\omega}(t)t\}\cos(\omega(t)t) \\ &\quad - \{\omega(t) + \dot{\omega}(t)t\}^2 \sin(\omega(t)t)], \end{aligned} \tag{2}$$

where z_0(m) is the amplitude of the base excitation and $\omega(t) \in \mathbb{R}$ is the frequency of the flapping wing in $\left(\frac{\mathrm{rad}}{\mathrm{s}}\right)$. Substitution of (2) into (1) generates

$$\begin{aligned} m_b\ddot{z}_b(t) + c\dot{z}_b(t) + kz_b(t) + (m_b + m_w)g \\ = z_0([c\{\omega(t) + \dot{\omega}(t)t\} \\ + m_w\{2\dot{\omega}(t) \\ + \ddot{\omega}(t)t\}]\cos(\omega(t)t) \\ + [k \\ - m_w\{\omega(t) \\ + \dot{\omega}(t)t\}^2]\sin(\omega(t)t)) + \bar{F}(t). \end{aligned} \tag{3}$$

Dividing equation (3) by m_b, defining damping ratio $\xi = \frac{c}{2m_b\omega_n}$ and natural frequency of the system $\omega_n = \sqrt{\frac{k}{m_b}}\left(\frac{\mathrm{rad}}{\mathrm{s}}\right)$, one could rewrite equation (3) as:

$$\begin{aligned} \ddot{z}_b(t) + 2\xi\omega_n\dot{z}_b(t) + \omega_n^2 z_b(t) \\ = z_0([2\xi\omega_n\{\omega(t) + \dot{\omega}(t)t\} \\ + \alpha\{2\dot{\omega}(t) + \ddot{\omega}(t)\}]\cos(\omega(t)t) \\ + [\omega_n^2 \\ - \alpha\{\omega(t) \\ + \dot{\omega}(t)t\}^2]\sin(\omega(t)t)) + F(t) \\ - (1 + \alpha)g, \end{aligned} \tag{4}$$

where $\alpha = \frac{m_w}{m_b}$ is the ratio of the mass of the wings to the base. Equation (4), equivalent dynamics of the vertical motion will be used to shape the state-space representation of the system in Section III.

III. Control Design of the Flapping-Wing Robot

The state vector of the system is selected as $\mathbf{x}(t) = [z_b(t), \dot{z}_b(t)]^T$, which transforms the second-order system (4) into state-space representation as (t is omitted in (5) for the sake of simplicity in presentation):

$$\begin{aligned} \dot{\mathbf{x}}(t) \\ = \begin{bmatrix} \dot{z}_b \\ -2\xi\omega_n\dot{z}_b - \omega_n^2 z_b + z_0 H + F - (1 + \alpha)g \end{bmatrix}, \end{aligned} \tag{5}$$

where

$$\begin{aligned} H(\omega(t), \dot{\omega}(t), \ddot{\omega}(t), t) \\ = [2\xi\omega_n\{\omega(t) + \dot{\omega}(t)t\} \\ + \alpha\{2\dot{\omega}(t) + \ddot{\omega}(t)\}]\cos(\omega(t)t) \\ + [\omega_n^2 - \alpha\{\omega(t) + \dot{\omega}(t)t\}^2]\sin(\omega(t)t). \end{aligned}$$

Based on Assumptions 1 and 2, which were taken from observation of the experiment data, the frequency of the flapping will change between the minimum and maximum bounds, $\omega_{\min} \le \omega(t) \le \omega_{\max}$ where $\omega_{\min} = 3.5(\mathrm{Hz})$ and $\omega_{\max} = 4.5(\mathrm{Hz})$. This small change in the frequency of the oscillation will ascend and descend the robot bird which means the elastic term and gravity are compensated indirectly by input lift force produced by flapping:

$$F(t) := kz_b(t) + (m_b + m_w)g + \tau(t), \tag{6}$$

in which $\tau(t)$ is a function:

$$\tau(t) = \frac{(\omega(t) - \omega_{\min})(p_{\max} - p_{\min})}{(\omega_{\max} - \omega_{\min}) + p_{\min}},$$

that maps $\omega(t)$ from range of $[21.9911, 28.2743]\left(\frac{\mathrm{rad}}{\mathrm{s}}\right)$ to the range of p in $[-0.5, 0.5]$.

Preprint version of the article: S. R. Nekoo and A. Ollero, "A Proportional Closed-loop Control for Equivalent Vertical Dynamics of Flapping-Wing Flying Robot," 2023 International Conference on Unmanned Aircraft Systems (ICUAS), Warsaw, Poland, 2023, pp. 1294-1300, doi: 10.1109/ICUAS57906.2023.10156070.

The next step is to define the position error of Z-axis as $e(t) = z_{\mathrm{b}}(t) - z_{\mathrm{b,des}}$ in which $z_{\mathrm{b,des}}(\mathrm{m})$ is the desired height of the regulation control, and introduce the proportional control law:

$$\omega(t) = -k_{\mathrm{p}} e(t) + \omega_0, \tag{7}$$

where k_{p} is a positive proportional gain of control law and ω_0 is a constant minimum flapping frequency that keeps the robot bird flying steadily in the air, which in our case, is the average value of the bounds of flapping $\omega_0 = 4(\mathrm{Hz}) = 25.1327\left(\frac{\mathrm{rad}}{\mathrm{s}}\right)$.

IV. Results

Similar to Fig. 2, the time of simulation was set $t_{\mathrm{f}} = 4(\mathrm{s})$. The initial condition was chosen $\mathbf{x}(0) = [1.2,0]^T$ and the desired condition is $\mathbf{x}(4) = [2,0]^T$. The analysis will be done for the robot without the leg-claw subsystem and manipulator, where most of the flight data are associated with that prototype. The total weight of the E-Flap robot was reported $510(\mathrm{g})$ [17]. Measuring the weight of the wings $m_{\mathrm{w}} = 150(\mathrm{g})$ and the rest of the body $m_{\mathrm{b}} = 360(\mathrm{g})$, result in weight ratio $\alpha = 0.4167$. The excitation of the wings due to flapping is transferred to the body of the robot through the carbon fiber tube of the wing. The tube acts like a clamped-free beam with equivalent stiffness constant:

$$k = \frac{3EI}{L^3}\left(\frac{\mathrm{N}}{\mathrm{m}}\right), \tag{8}$$

where $E = 65 \times 10^9 \left(\frac{\mathrm{N}}{\mathrm{m}^2}\right)$ is the elastic modulus of carbon fiber, length of the wing is $a = 0.75(m)$, which defines $L = 0.25(\mathrm{m})$ as the distance between the CoM of the body and effective lift force on the wing, $I = 5.1051 \times 10^{-11}(\mathrm{m}^4)$ is the second moment of the cross-sectional area of the tube, with an inner diameter of 4 and an outer diameter of $6(\mathrm{mm})$. This ultimately results in $k = 637.115\left(\frac{\mathrm{N}}{\mathrm{m}}\right)$. The stiffness constant generates the natural frequency of the flapping robot as $\omega_{\mathrm{n}} = 42.0686\left(\frac{\mathrm{rad}}{\mathrm{s}}\right)$. Selection of the damping ratio as $\xi = 0.011$, the damping coefficient is found $c = 2m_{\mathrm{b}}\omega_{\mathrm{n}}\xi = 0.3332\left(\frac{\mathrm{Ns}}{\mathrm{m}}\right)$ which results in matching the simulation output with the experimental data. The control gain of the input law is chosen as $k_{\mathrm{p}} = 4$. The position of the robot in Z-axis presented in Fig. 4. The velocity state is illustrated in Fig. 5 and the input signal, and flapping frequency are plotted in Fig. 6. Finally, the error is plotted in Fig. 7.

To check the performance of the controller with a different final condition, a set of desired heights were selected for simulating the controller and the equivalent system dynamics

$$Z_{\mathrm{des}} = \{0.25,0.5,0.75,1,1.25,1.5,1.75,2,2.5\}(\mathrm{m}),$$

which results in Fig. 8, successfully regulated to zero error. The oscillation in the whole trajectory which was caused by the flapping could be observed in the results, similar to experimental data which shows the validity of the simulation.

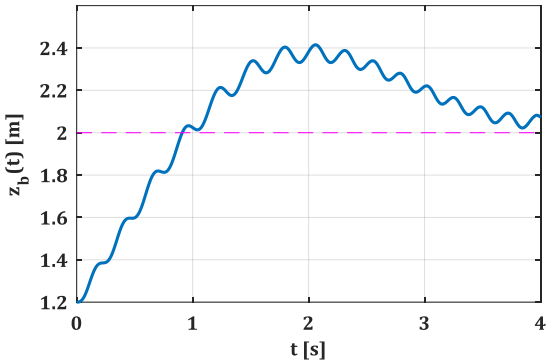

Fig. 4. The position state of the modeled equivalent dynamics.

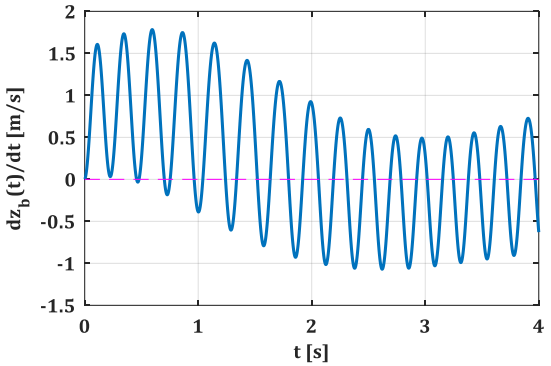

Fig. 5. The velocity state of the modeled equivalent dynamics.

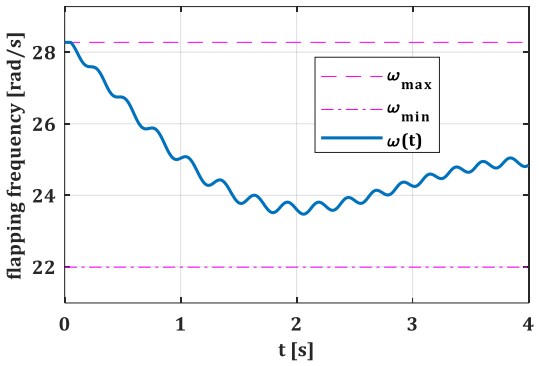

Fig. 6. Flapping frequency of the system, as the input to the control problem.

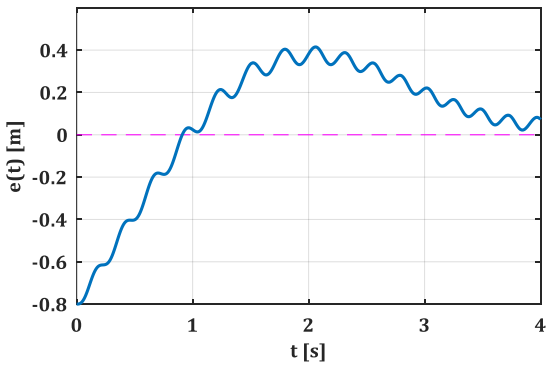

Fig. 7. Error of the system.

Preprint version of the article: S. R. Nekoo and A. Ollero, "A Proportional Closed-loop Control for Equivalent Vertical Dynamics of Flapping-Wing Flying Robot," 2023 International Conference on Unmanned Aircraft Systems (ICUAS), Warsaw, Poland, 2023, pp. 1294-1300, doi: 10.1109/ICUAS57906.2023.10156070.

Transient or steady-state flight: This is an important discussion on the flight control of the flapping-wing robot. The dynamic of the FWFR is a slow system and it needs several seconds to pass the transient condition of the system. The Opti-track testbed of the GRVC laboratory allows us to experiment within a diagonal line, less than 15(m) which almost takes less than 3 to 4 seconds for the robot to reach the end and perch on the branch, see Fig. 9 . If we increase the time of simulation with the same condition and control gain, the behavior of the system is found in Fig. 10. It is clear that the system needs more than 8 seconds to reach the steady-state condition and the control design is usually done based on that. So, one could see that the defined gain $k_{\mathrm{p}} = 4$ is not regulating the system to desired conditions 0.25 and 0.5(m). Reducing the gain to $k_{\mathrm{p}} = 3$ will solve the problem and also regulates the system successfully to all desired conditions. However, at a critical impact point to the branch, around 4 seconds, the error would increase. This is a drawback that forced the control designer to define the gain based on transient conditions, imposed by the physical limitation of the flight zone.

Another point is the selection of only a proportional controller. With the same consideration, if one used a proportional-integral (PI) controller to omit the steady-state error after 8 seconds, please see Fig. 10, the error at 4 seconds would increase again. However, with the PI design, considering $k_{\mathrm{p}} = 3$ and $k_{\mathrm{i}} = 0.5$, the shift in the steady-state error is corrected, presented in Fig. 11. The overall discussion and results show a significant point in the design of the controller for the FWFR. It also indicates that moving towards more model-based advanced controllers is not trivial since the robot is working in the transient flight zone caused by the slow dynamics of the robot and physical limitation of the GRVC testbed.

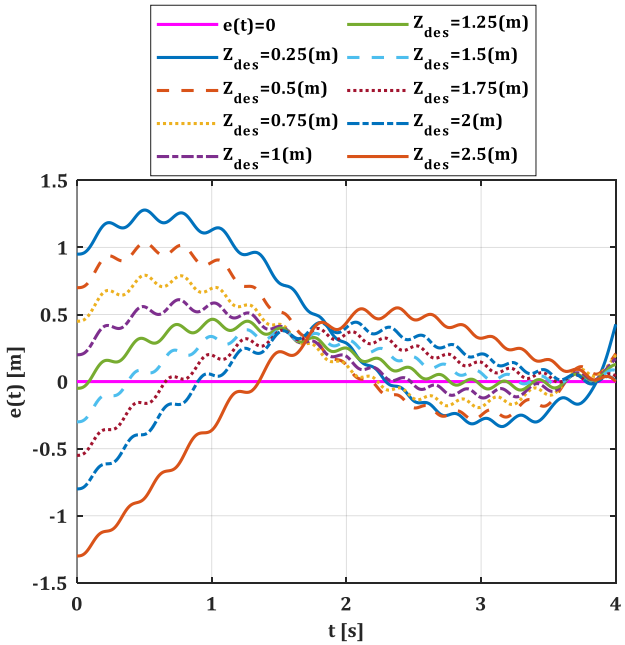

Fig. 8. Error of the system with the different final conditions.

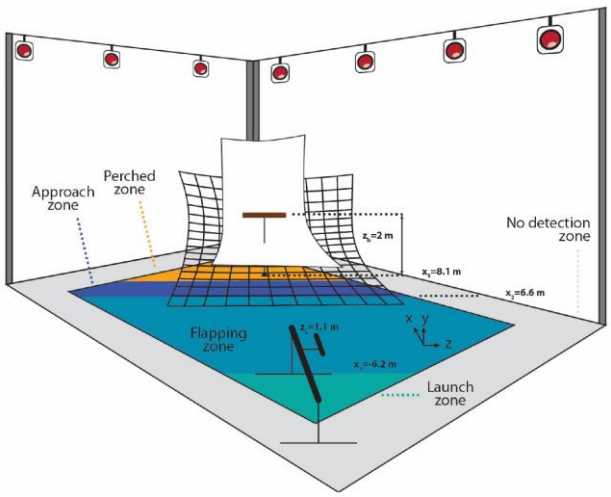

Fig. 9. The Opti-track testbed of the GRVC and the different zones of flight [1].

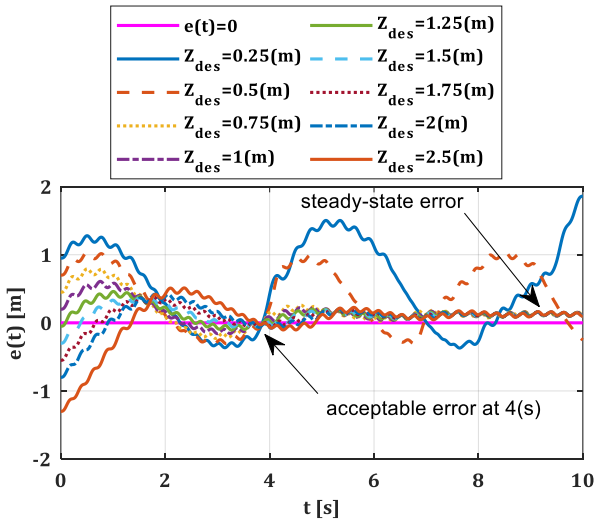

Fig. 10. Error of the system with the different final conditions, increased time to 10 seconds.

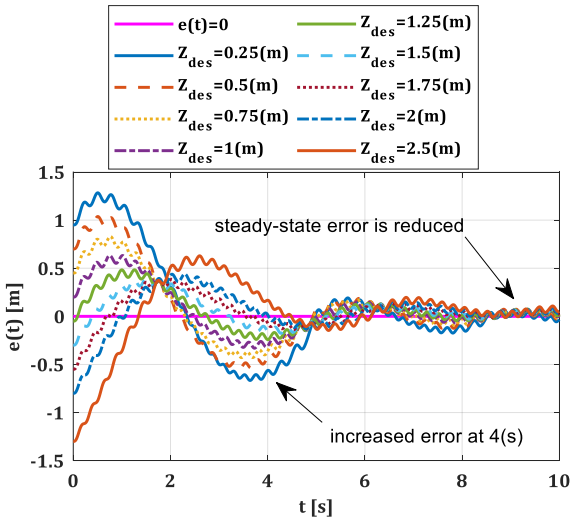

Fig. 11. Error of the system with PI controller.

Preprint version of the article: S. R. Nekoo and A. Ollero, "A Proportional Closed-loop Control for Equivalent Vertical Dynamics of Flapping-Wing Flying Robot," 2023 International Conference on Unmanned Aircraft Systems (ICUAS), Warsaw, Poland, 2023, pp. 1294-1300, doi: 10.1109/ICUAS57906.2023.10156070.

V. Conclusions

The flapping-wing robotic systems have become an interesting topic for flight control and applications such as manipulation, perching on a branch, monitoring, and inspection by cameras, etc. Flight control is an important step in the design and prototyping as well. This paper focused on the control of the equivalent dynamics of vertical motion using a proportional closed-loop design. The equivalent dynamics have been adopted from vibration models subjected to base excitation that generates oscillation in motion. Those oscillations here in this work were generated by the flapping of the wings and disturbed the body of the robot during the flight. A model and control approach was proposed and simulated here to analyze the behavior of the motion and compared the results with the available experimental data. The results showed similarity and validated the equivalent modeling. The simple proportional linear control was chosen to keep the design as simple as possible for having a clear understanding of the motion analysis and oscillatory behavior of the dynamics. A discussion on the transient and steady-state flight has been presented that showed the reason for choosing the simple proportional controller in this work.

Acknowledgment

This work was supported by the European Project GRIFFIN ERC Advanced Grant 2017, Action 788247; and HAERA (Spanish Ministry of Science and Innovation PID2020-119027RB-I00).

References

[1] R. Zufferey, J. T. Barbero, D. F. Talegon, S. R. Nekoo, J. A. Acosta, and A. Ollero, "How ornithopters can perch autonomously on a branch," *Nature Communications*, vol. 13, pp. 1-11, 2022.

[2] P. Chirarattananon, K. Y. Ma, and R. J. Wood, "Perching with a robotic insect using adaptive tracking control and iterative learning control," *The International Journal of Robotics Research*, vol. 35, pp. 1185-1206, 2016.

[3] M. A. Graule, P. Chirarattananon, S. B. Fuller, N. T. Jafferis, K. Y. Ma, M. Spenko, *et al.*, "Perching and takeoff of a robotic insect on overhangs using switchable electrostatic adhesion," *Science*, vol. 352, pp. 978-982, 2016.

[4] S. Ryu, U. Kwon, and H. J. Kim, "Autonomous flight and vision-based target tracking for a flapping-wing MAV," in *2016 IEEE/RSJ International Conference on Intelligent Robots and Systems (IROS)*, Daejeon, Korea (South), 2016, pp. 5645-5650.

[5] W. Ding, Z. Liu, F. Zhang, L. Cui, and S. Wang, "Research on visual image processing and edge detection method of micro flapping wing flying robot based on cluster analysis," in *Seventh Asia Pacific Conference on Optics Manufacture and 2021 International Forum of Young Scientists on Advanced Optical Manufacturing (APCOM and YSAOM 2021)*, 2022, pp. 493-500.

[6] H. Huang, W. He, J. Wang, L. Zhang, and Q. Fu, "An all servo-driven bird-like flapping-wing aerial robot capable of autonomous flight," *IEEE/ASME Transactions on Mechatronics*, vol. 27, pp. 5484-5494, 2022.

[7] A. Gómez Eguíluz, J. P. Rodríguez Gómez, R. Tapia, F. J. Maldonado, M.-d. D. R., J. A. Acosta, *et al.*, "Why fly blind? Event-based visual guidance for ornithopter robot flight," in *International Conference on Intelligent Robots and Systems (IROS 2021)*, Prague, Czech Republic, 2021.

[8] J. P. Rodríguez-Gómez, R. Tapia, M. M. G. Garcia, J. R. Martínez-de Dios, and A. Ollero, "Free as a bird: Event-based dynamic sense-and-avoid for ornithopter robot flight," *IEEE Robotics and Automation Letters*, vol. 7, pp. 5413-5420, 2022.

[9] X. Wu, W. He, Q. Wang, T. Meng, X. He, and Q. Fu, "A long-endurance flapping-wing robot based on mass distribution and energy consume method," *IEEE Transactions on Industrial Electronics*, 2022.

[10] Z. Ren, S. Kim, X. Ji, W. Zhu, F. Niroui, J. Kong, *et al.*, "A high‐lift micro‐aerial‐robot powered by low‐voltage and long‐endurance dielectric elastomer actuators," *Advanced Materials*, vol. 34, p. 2106757, 2022.

[11] S. R. Nekoo, D. Feliu-Talegon, J. A. Acosta, and A. Ollero, "A 79.7 g manipulator prototype for E-Flap robot: A plucking-leaf application," *IEEE Access*, vol. 10, pp. 65300-65308, 2022.

[12] A. E. Gomez-Tamm, V. Perez-Sanchez, B. C. Arrue, and A. Ollero, "SMA actuated low-weight bio-inspired claws for grasping and perching using flapping wing aerial systems," in *2020 IEEE/RSJ International Conference on Intelligent Robots and Systems (IROS)*, Las Vegas, NV, USA, 2020, pp. 8807-8814.

[13] A. A. Paranjape, S.-J. Chung, and J. Kim, "Novel dihedral-based control of flapping-wing aircraft with application to perching," *IEEE Transactions on Robotics*, vol. 29, pp. 1071-1084, 2013.

[14] F. Fei, Z. Tu, and X. Deng, "An at-scale tailless flapping wing hummingbird robot. II. Flight control in hovering and trajectory tracking," *Bioinspiration & Biomimetics*, 2022.

[15] H. Gao, J. Hu, D. Liu, and J. Zhu, "Adaptive vibration control for two-stage bionic flapping wings based on neural network algorithm," in *2022 41st Chinese Control Conference (CCC)*, Hefei, China, 2022, pp. 3539-3544.

[16] F. J. Maldonado, J. A. Acosta, J. Tormo-Barbero, P. Grau, M. M. Guzman, and A. Ollero, "Adaptive nonlinear control for perching of a bioinspired ornithopter," in *2020 IEEE/RSJ International Conference on Intelligent Robots and Systems (IROS)*, 2020, pp. 1385-1390.

[17] R. Zufferey, J. Tormo-Barbero, M. M. Guzmán, F. J. Maldonado, E. Sanchez-Laulhe, P. Grau, *et al.*,

"Design of the high-payload flapping wing robot E-Flap," *IEEE Robotics and Automation Letters*, vol. 6, pp. 3097-3104, 2021.

[18] S. R. Nekoo, J. Á. Acosta, and A. Ollero, "Combination of terminal sliding mode and finite-time state-dependent Riccati equation: Flapping-wing flying robot control," *Proceedings of the Institution of Mechanical Engineers, Part I: Journal of Systems and Control Engineering*, p. 09596518221138627, 2022.

[19] F. Müller, L. Woiwode, J. Gross, M. Scheel, and M. Krack, "Nonlinear damping quantification from phase-resonant tests under base excitation," *Mechanical Systems and Signal Processing*, vol. 177, p. 109170, 2022.

[20] S. G. Kelly, *Mechanical vibrations: theory and applications*: Cengage learning Stamford, USA, 2012.

[21] X. Guo, P. Gao, H. Ma, H. Li, B. Wang, Q. Han, *et al.*, "Vibration characteristics analysis of fluid-conveying pipes concurrently subjected to base excitation and pulsation excitation," *Mechanical Systems and Signal Processing*, vol. 189, p. 110086, 2023.

[22] A. Mohanty and R. K. Behera, "Energy harvesting from a cantilever beam with a spring-loaded oscillating mass system and base excitation," *Proceedings of the Institution of Mechanical Engineers, Part K: Journal of Multi-body Dynamics*, p. 14644193221135929, 2022.

[23] N. N. Linh, V. A. Tuan, N. V. Tuan, and N. D. Anh, "Response analysis of undamped primary system subjected to base excitation with a dynamic vibration absorber integrated with a piezoelectric stack energy harvester," *Vietnam Journal of Mechanics*, vol. 44, pp. 490-499, 2022.

[24] T. Dong, W.-G. Zhang, and Y. Liu, "Dynamic snap-through phenomena and nonlinear vibrations of bistable asymmetric cross-ply composite-laminated square plates with two potential wells under center base excitation," *The European Physical Journal Special Topics*, vol. 231, pp. 2199-2209, 2022.